

<Technical Note>

A Compilation and Evaluation of Thermal and Mechanical Properties of Bentonite-based Buffer Materials for a High-level Waste Repository

Won-Jin Cho, Jae-Owan Lee, and Chul-Hyung Kang

Korea Atomic Energy Research Institute
150 Dukjin-dong, Yusong-gu, Taejeon 305-353, Korea
E-mail : wjcho@kaeri.re.kr

(Received August 17, 2001)

Abstract

The thermal and mechanical properties of compacted bentonite and bentonite-sand mixture were collected from the literatures and compiled. The thermal conductivity of bentonite is found to increase almost linearly with increasing dry density and water content of the bentonite. The specific heat can also be expressed as a function of water content, and the coefficient of thermal expansion is almost independent on the dry density. The logarithm of unconfined compressive strength and Young's modulus of elasticity increase linearly with increasing dry density, and in the case of constant dry density, it can be fitted to a second order polynomial of water content. Also the unconfined compressive strength and Young's modulus of elasticity of the bentonite-sand mixture decreases with increasing sand content. The Poisson's ratio remains constant at the dry density higher than 1.6 Mg/m^3 , and the shear strength increases with increasing dry density.

Key Words : mechanical property, thermal property, compacted bentonite, buffer material, high-level waste repository

1. Introduction

A repository for high-level radioactive wastes would be constructed in the bedrock at a depth of several hundred meters below the ground surface. The repository would be expected to be of room-and-pillar design, and the waste containers would be deposited in an array of large-diameter boreholes drilled on the floors of the emplacement rooms. After the emplacement of a waste container, the gap between the container and the

wall of the borehole would be filled with a buffer material. The buffer has to dissipate the decay heat from waste into the surrounding rock to avoid the possibility of thermal stress on the container and the waste form, and also has to protect the container and waste from the external mechanical stress. Therefore the buffer material should have good thermal and mechanical properties to assure the long-term integrity of the engineered barriers in the repository.

Present design concepts [1,2] of a repository in

a granite formation include the use of compacted clay-based materials as a buffer, and the compacted bentonite and bentonite-sand mixture have been suggested as a candidate buffer material. Therefore the thermal and mechanical properties of the compacted bentonite and the mixture of bentonite and sand are required to assess the performance of engineered barriers in a high-level waste repository. In Korea, Cho et al. [3] reported the mechanical properties of Kyungju bentonite which is produced from tertiary sediments in eastern coastal area of Kyungsangbuk-do. As the investigation was however intended to assess the possible use of Kyungju bentonite as a buffer material, the limited numbers of measurement were conducted and furthermore the thermal properties were not considered. Therefore the additional thermal and mechanical properties of bentonite-based material are necessary for the performance assessment of the engineered barriers. These properties can be ideally obtained from the extensive direct measurement for the domestic bentonite. The direct measurement is however a time and cost consuming process, and may not be appropriate at the early stage that requires the comparative analysis of various design alternatives for the engineered barriers to establish the reference concept of a geological repository. In this study, as an alternative, the thermal and mechanical properties of the compacted bentonite and the bentonite-sand mixture were collected from the literatures and compiled. These data were analyzed and evaluated to provide the typical values of the thermal and mechanical properties for the performance assessment of engineered barriers.

2. Thermal Properties

The thermal properties of buffer material

determine the capability of buffer to dissipate the decay heat from waste into the surrounding rock. Here, the thermal conductivity, the specific heat and the coefficient of thermal expansion for the bentonite and bentonite-sand mixture are collected and analyzed.

2.1. Thermal Conductivity

The thermal conductivity of the compacted bentonite depends generally on the dry density, the water content and the measuring temperature [4,5]. The thermal conductivity tends to increase with increasing temperature. However the repository is designed to maintain the maximum temperature in the buffer below 100°C, and no significant change in the thermal conductivity of the compacted bentonite was observed for the temperature range up to 100°C [5].

The collected thermal conductivity data are mainly for the compacted bentonite, and some data for the bentonite-sand mixture are also included [4-15]. The dry densities are in the range of 1.2 Mg/m³ to 2.0 Mg/m³, and the water contents are varied from dry condition to saturated condition. The thermal conductivity of compacted bentonite is found to increase with increasing dry density in the case of constant water content. This behavior is due to the decrease of interparticle void space resulting in the improvement of heat conduction. When the dry density is constant, the thermal conductivity of bentonite shows strong dependence on the water content, and increases with increasing water content. As the water content increases, air in the void space of bentonite is replaced by water with higher thermal conductivity. Also the swelling of bentonite gives the better contact between bentonite particles and seals the probable cracks in bentonite block. Then the thermal conductivity increases. The regression analysis using the least squares fit technique shows

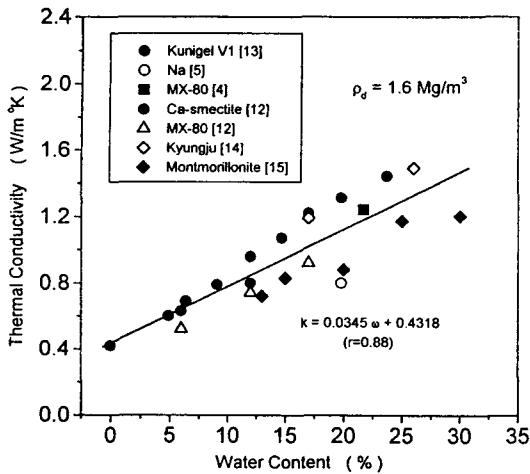


Fig. 1. Thermal Conductivity of the Compacted Bentonite with Dry Density of 1.6 Mg/m³ Versus the Water Content

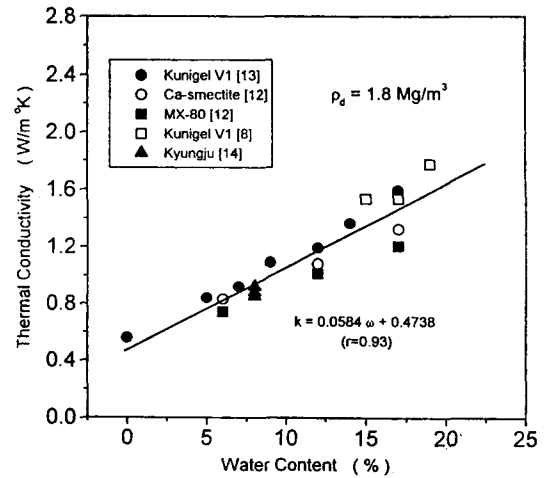


Fig. 2. Thermal Conductivity of the Compacted Bentonite with Dry Density of 1.8 Mg/m³ Versus the Water Content

that the thermal conductivity increases almost linearly with increasing water content (Fig. 1, Fig. 2), and the correlations can be expressed as follows:

- dry density: 1.2 Mg/m³
 $k = 0.0236 \omega + 0.1699 \quad (r=0.98) \quad (1a)$

- dry density: 1.4 Mg/m³
 $k = 0.0306 \omega + 0.2286 \quad (r=0.95) \quad (1b)$

- dry density: 1.6 Mg/m³
 $k = 0.0345 \omega + 0.4318 \quad (r=0.88) \quad (1c)$

- dry density: 1.8 Mg/m³
 $k = 0.0584 \omega + 0.4738 \quad (r=0.93) \quad (1d)$

- dry density: 2.0 Mg/m³
 $k = 0.0545 \omega + 0.7219 \quad (r=0.83) \quad (1e)$

where k is thermal conductivity (W/m °K) and ω is water content (%).

The thermal conductivity of bentonite-sand mixture increases linearly with an increase in sand content in the case of constant dry density and water content, although its degree of increase depends on the dry density of mixture [26]. This

behavior is due to the high interparticle density and better conductance at the interparticle contacts of the mixture.

2.2. Specific Heat

The influence of temperature on the specific heat seems to be insignificant. The specific heat of the bentonite with a dry density of 1.8 Mg/m³ shows a slight dependence on temperature, and is in the range of 0.2 to 0.4 kJ kg⁻¹ K⁻¹ when the measuring temperatures are varied from 20 to 100 °C [7]. Therefore under the repository condition that the maximum temperature is maintained below 100 °C, the specific heat can be assumed to be independent of the temperature. The specific heat of bentonite is almost independent on the dry density (Fig. 3). The specific heat of the bentonite and bentonite-sand mixture can be determined by summing up the products of the specific heat and specific unit weight for each component. The compacted bentonite or the bentonite-sand mixture contains a

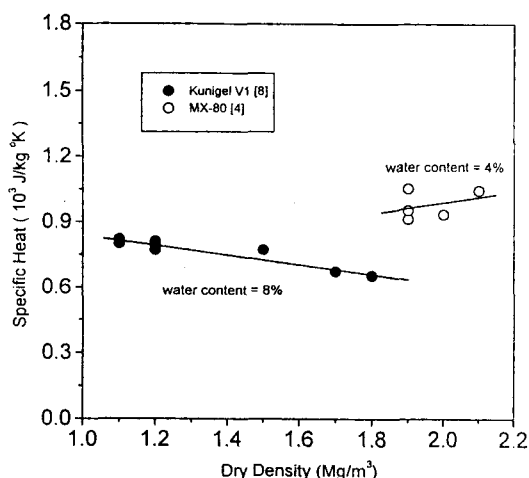


Fig. 3. Change in the Specific Heat of the Compacted Bentonite with Increasing Dry Density

solid phase (bentonite or bentonite-sand), air and water in voids, and then the specific heat can be represented by the following equation:

$$c = \gamma_s c_s + \gamma_w c_w + \gamma_a c_a \quad (2)$$

where c and γ are specific heat and specific unit weight, and the subscript s , w and a represent solid, water and air, respectively. The term for air phase has a negligibly small value compared with the others, and the specific heat of solid phase will be as same as that at a water content of 0%. As the specific heat at the water content of 0% is $0.323 \text{ kJ kg}^{-1} \text{ K}^{-1}$ for the bentonite with a dry density of 1.8 Mg/m^3 , and $0.341 \text{ kJ kg}^{-1} \text{ K}^{-1}$ for the bentonite-sand mixture with a dry density of

1.6 Mg/m^3 [7]. Therefore the specific heat of buffer material as a function of water content, can be represented by the following equations :

- Bentonite with a dry density of 1.8 Mg/m^3
 $c = (32.3 + 4.18 w)/(100 + w) \quad (3a)$

- Bentonite-sand (70:30) mixture with a dry density of 1.6 Mg/m^3
 $c = (34.1 + 4.18 w)/(100 + w) \quad (3b)$

where c is specific heat ($\text{kJ kg}^{-1} \text{ K}^{-1}$), w is water content (%). The estimated specific heat using Eq.(3) agrees well with the measured values [7].

2.3. Coefficient of Thermal Expansion

The Coefficients of thermal expansion for the compacted bentonite are reported only by Börgesson et al. [11], and are presented in Table 1. They were measured at the temperature range of 20°C to 60°C . As shown in the table, the coefficient of thermal expansion decreases with increasing dry density under the measuring condition, but no significant difference is observed. Therefore the coefficient of thermal expansion can be assumed to be constant for the buffer material in the repository.

3. Mechanical Properties

The mechanical properties of buffer material are required to assess the ability of buffer to support the container and waste from the external

Table 1. Coefficient of Thermal Expansion of the Compacted Bentonite

Bentonite	Dry Density (Mg/m³)	Water Content (%)	Coefficient of Thermal Expansion ($1/^\circ\text{K}$)	Temperature Range	Ref.
MX-80	1.2	13	3.1×10^{-4}	20 - 60 °C	11
	1.5	33	3.0×10^{-4}		
	1.65	27	2.2×10^{-4}		

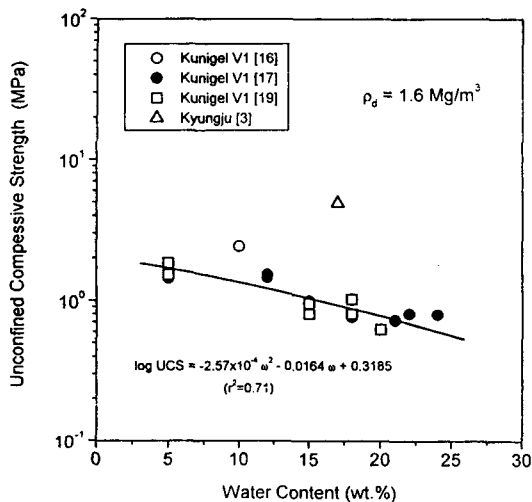


Fig. 4. Change in the Unconfined Compression Strength of the Compacted Bentonite with Increasing Water Content (dry density: 1.6 Mg/m³)

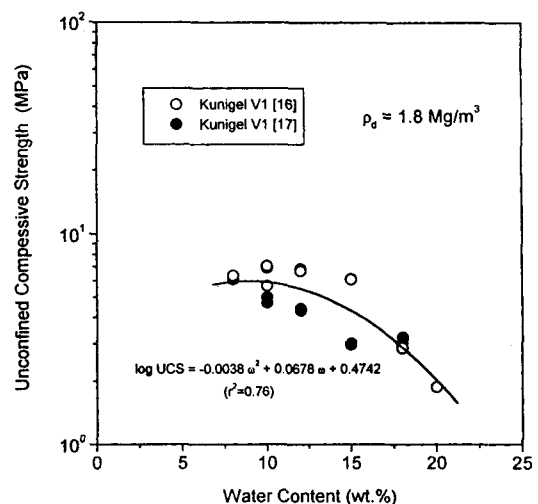


Fig. 5. Change in the Unconfined Compression Strength of the Compacted Bentonite with Increasing Water Content (dry density: 1.8 Mg/m³)

mechanical stress. Here unconfined compression strength, Young's modulus of elasticity, Poisson's ratio, shear strength and consolidation properties of the bentonite and bentonite-sand mixture are collected and analyzed.

3.1. Unconfined Compression Strength

The specimen is compressed uniaxially by applying constant strain rate without radial confinement, and the axial stress at the failure of specimen is an unconfined compression strength.

The collected unconfined compression strength data are mainly for the compacted bentonite, and some data for the bentonite-sand mixture are also included [3,16-19]. The unconfined compression strength of the bentonite increases with increasing dry density. For example, the unconfined compression strength-dry density relationship for bentonite at a water content of 10% can be approximated as:

$$\log \text{UCS} = 1.6745 \rho_d - 2.2960 \quad (r = 0.96) \quad (4)$$

where UCS is the unconfined compression strength (MPa), and ρ_d is the dry density (Mg/m³). At constant dry density, the unconfined compression strength of bentonite is disposed to decrease with increasing water content. As shown in Fig. 4 and 5, the relationship between the logarithm of unconfined compression strength and the water content of bentonite can be fitted to a line using the least squares fit technique :

- dry density: 1.4 Mg/m³
 $\log \text{UCS} = 5.38 \times 10^{-4} \omega^2 - 0.0454 \omega + 0.3235$
 $(r^2 = 0.81) \quad (5a)$

- dry density: 1.6 Mg/m³
 $\log \text{UCS} = -2.57 \times 10^{-4} \omega^2 - 0.0164 \omega + 0.3185$
 $(r^2 = 0.71) \quad (5b)$

- dry density: 1.8 Mg/m³
 $\log \text{UCS} = -0.0038 \omega^2 + 0.0678 \omega + 0.4742$
 $(r^2 = 0.76) \quad (5c)$

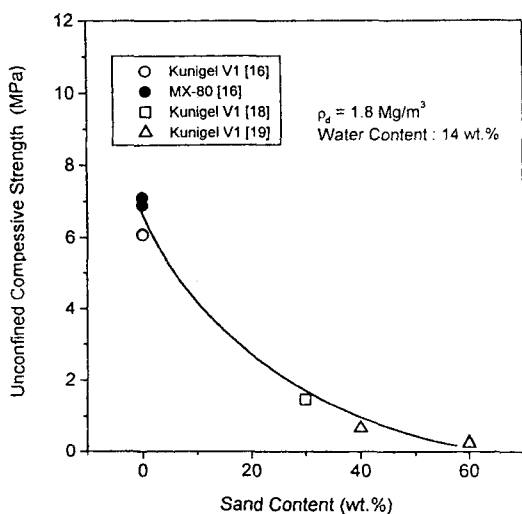


Fig. 6. Effect of Sand Content on the Unconfined Compression Strength of the Bentonite-Sand Mixture

where UCS is the unconfined compression strength (MPa), and ω is water content (%). In Fig. 4, the data for Kyungju bentonite show considerable deviation from the trend of other data, and it might be due to the difference of swelling capacity between Ca-bentonite and Na-bentonite. Therefore these data are not included to obtain Eq. (5b). For the bentonite-sand mixture, the unconfined compression strength drops significantly with increasing sand content when dry density and water content are constant (Fig. 6). This may be due to the reduction of interparticle binding force with increasing sand content. When the sand content is 30 wt.%, the unconfined compression strength of the bentonite-sand mixture with dry density of 1.6 Mg/m³ and 1.8 Mg/m³ can be approximated by following equation using the least squares fit technique (Fig. 7)

- dry density: 1.6 Mg/m³ (sand content: 30 wt.%)
 $\log \text{UCS} = 0.0020 \omega^2 - 0.0930 \omega + 0.4289$
 $(r^2=0.67)$ (6a)

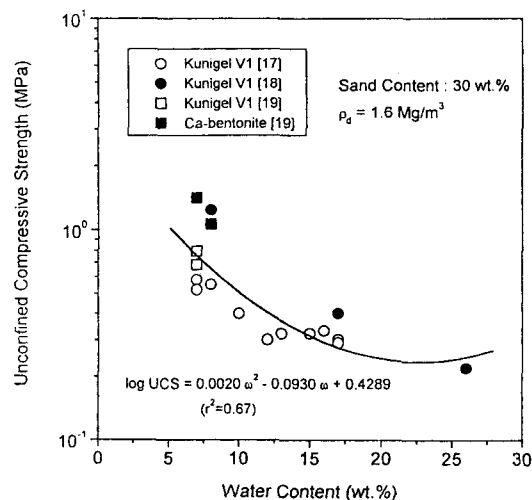


Fig. 7. Unconfined Compression Strength of the Bentonite-Sand Mixture (70:30) with Dry Density of 1.6 Mg/m³ versus the Water Content

- dry density: 1.8 Mg/m³ (sand content: 30 wt.%)
 $\log \text{UCS} = -0.0027 \omega^2 + 0.0107 \omega + 0.5702$
 $(r^2=0.99)$ (6b)

3.2. Young's Modulus of Elasticity

The Young's modulus of elasticity is defined as the ratio between uniaxial stress and axial strain.

The collected Young's modulus of elasticity data are mainly for the compacted bentonite, and some data for the bentonite-sand or bentonite-crushed rock mixture are also included [3,16-19]. The dependence of the Young's modulus of elasticity of bentonite on the dry density and water content is very similar to that of unconfined compression strength. The logarithm of the Young's modulus of elasticity also increases with increasing dry density when the water content is constant. At the water content of 10%, the relationship between the dry density of bentonite and the Young's modulus of elasticity can be fitted to a straight line expressed as follows:

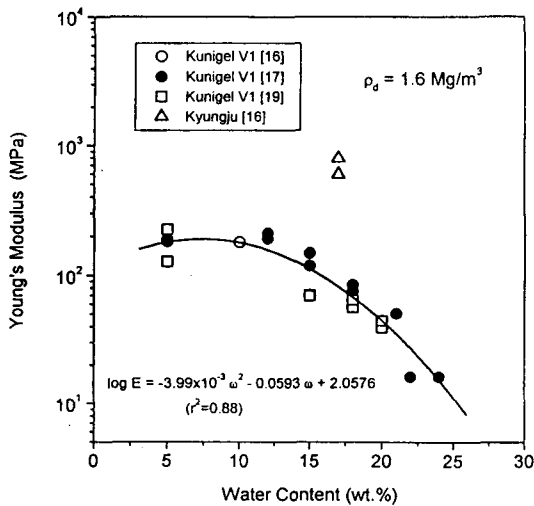


Fig. 8. Change in the Young's Modulus of Elasticity of the Compacted Bentonite with Increasing Water Content (dry density: 1.6 Mg/m³)

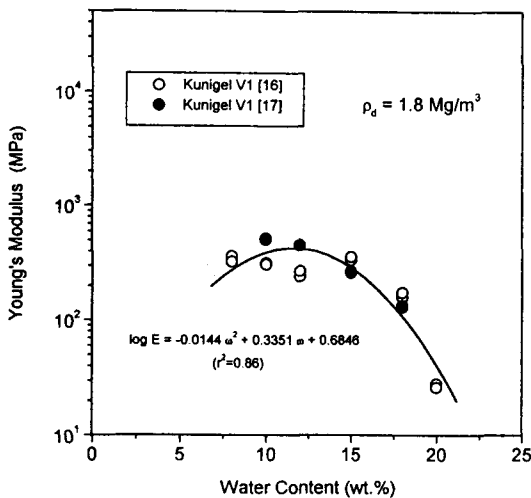


Fig. 9. Change in the Young's Modulus of Elasticity of the Compacted Bentonite with Increasing Water Content (dry density: 1.8 Mg/m³)

$$\log E = 1.5029 \rho_d - 0.1822 \quad (r = 0.92) \quad (7)$$

where E is the Young's modulus of elasticity ($\times 10^2$ MPa), and ρ_d is the dry density of bentonite (Mg/m^3). At the constant dry density, the Young's modulus of elasticity tends to decrease with increasing water content. As shown in Fig. 8 and 9, using the least squares fit technique the relationship between the Young's modulus of elasticity and the dry density of bentonite can be expressed as :

- dry density: 1.4 Mg/m^3
 $\log E = 0.0038 \omega^2 - 0.1433 \omega + 2.8578$
 $(r^2 = 0.87)$ (8a)

- dry density: 1.6 Mg/m^3
 $\log E = -3.99 \times 10^{-3} \omega^2 + 0.0593 \omega + 2.0576$
 $(r^2 = 0.88)$ (8b)

- dry density: 1.8 Mg/m^3
 $\log E = -0.0144 \omega^2 + 0.3351 \omega + 0.6846$
 $(r^2 = 0.86)$ (8c)

where E is the Young's modulus of elasticity ($\times 10^2$ MPa), ω is the water content (%). In Fig. 8, the data for Kyungju bentonite show considerable deviation from the trend of other data, and it might be due to the difference of swelling capacity between Ca-bentonite and Na-bentonite. Therefore these data are not included to obtain Eq. (8b).

For the bentonite-sand mixture, when the dry density and water content are constant, the Young's modulus of elasticity decrease sharply with increasing sand content (Fig. 10). This behavior is similar to that of the unconfined compression strength. When the sand content is 30 wt.%, the Young's modulus of elasticity of the bentonite-sand mixture with dry density of 1.6 Mg/m^3 and 1.8 Mg/m^3 can be approximated by following equation (Fig. 11):

- dry density: 1.6 Mg/m^3 (sand content: 30 wt.%)
 $\log E = 8.83 \times 10^{-4} \omega^2 - 0.0730 \omega + 2.3751$
 $(r^2 = 0.66)$ (9a)

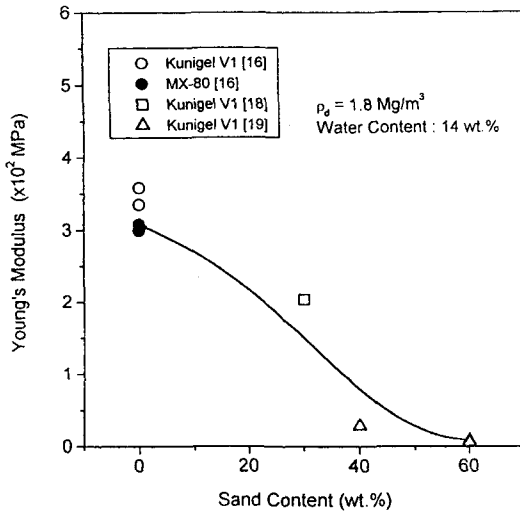


Fig. 10 Effect of Sand Content on the Young's Modulus of Elasticity of the Bentonite-Sand Mixture

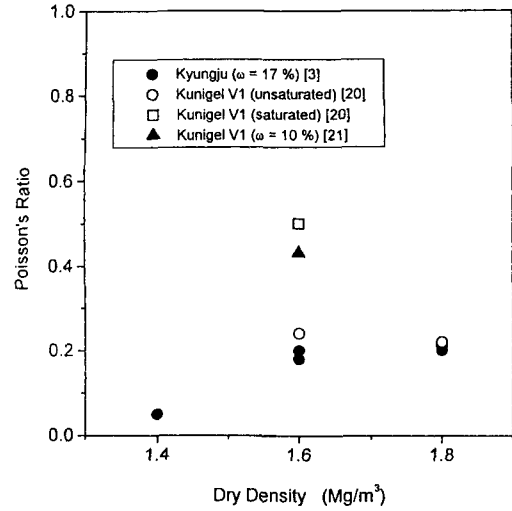


Fig. 12. Poisson's Ratio of the Compacted Bentonite

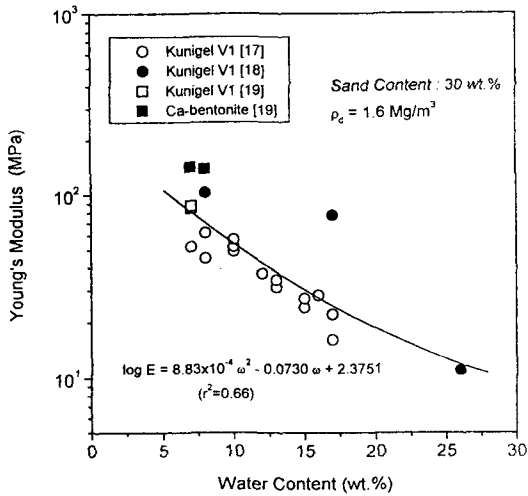


Fig. 11. Young's Modulus of Elasticity of the Bentonite-Sand Mixture (70:30) with Dry Density of 1.6 Mg/m³ Versus the Water Content

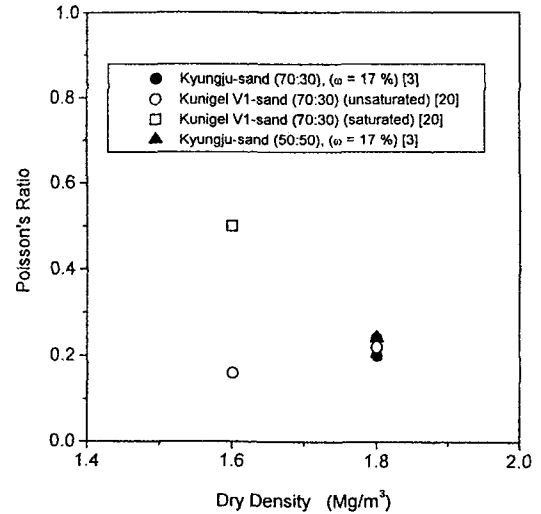


Fig. 13. Poisson's Ratio of the Bentonite-sand Mixture

• dry density: 1.8 Mg/m³ (sand content: 30 wt.%)

$$\log E = -0.0109 \omega^2 + 0.2036 \omega + 1.5275$$

$$(r^2=0.99) \quad (9b)$$

3.3. Poisson's Ratio

Poisson's ratio is the ratio between an axial strain and a lateral strain such that

Table 2. Shear Properties of the Compacted Bentonite

Bentonite	Dry Density (Mg/m ³)	Water Content (%)	Cohesion (kPa)	Angle of Friction (°)	Measuring Technique	Conditions	Ref.
Montmorillonite	1.3	10	80	39	triaxial	$\sigma_3=50\text{kPa}$	22
MX-80	1.3	42	40	8.8	simple shear	$200\text{kPa}<\sigma_N<2000\text{kPa}$	23
Montmorillonite	1.4	10	80	39	triaxial	$\sigma_3=50\sim300\text{kPa}$	22
Kyungju	1.4	17	500	27	triaxial	$\sigma_3=100\sim400\text{kPa}$	3
MX-80	1.4	37	150 0	7 13	triaxial triaxial	$\sigma_3>1000\text{kPa}$ $\sigma_3\leq1000\text{kPa}$	23
Ca-Bentonite	1.4	33	50 50 0 0	4.4 5.2 22 28	triaxial simple shear triaxial simple shear	$\sigma_3>200\text{kPa}$ $\sigma_N>200\text{kPa}$ $\sigma_3\leq200\text{kPa}$ $\sigma_N\leq200\text{kPa}$	24
Ca-Bentonite	1.5	29	80	6.4	direct shear	$\sigma_N>800\text{kPa}$	24
Montmorillonite	1.6	9	160~200	47~45	triaxial	$\sigma_3=50\sim300\text{kPa}$	22
Kunigel V1	1.6	10	120	10.3	triaxial		21
Ca-bentonite	1.6	10	110	8.5	triaxial	$\sigma_3=490\sim980\text{kPa}$	21
Kyungju	1.6	17	1000	37	triaxial	$\sigma_3=100\sim400\text{kPa}$	3
Montmorillonite	1.7	8	440	45	triaxial	$\sigma_3=50\sim300\text{kPa}$	22
Kyungju	1.8	17	1100	50	triaxial	$\sigma_3=100\sim400\text{kPa}$	3

$$\mu = -\epsilon_x / \epsilon_z = -\epsilon_y / \epsilon_z \quad (10)$$

where μ is Poisson's ratio, ϵ_x , ϵ_y , ϵ_z are the strains in the x, y, z directions, respectively.

The Poisson's ratio for the bentonite and bentonite-sand mixture were collected from the literatures[3,20,21]. The Poisson's ratio depends on dry density and water content. The relationship

between Poisson's ratio and dry density is shown in Fig. 12 and 13. As shown in the figures, the Poisson's ratio increases with an increase of dry density from 1.4 Mg/m³ to 1.6 Mg/m³, and then in the range of 1.6 Mg/m³ to 1.8 Mg/m³, both bentonite and bentonite-sand mixture show similar values of Poisson's ratio. That is, the Poisson's ratio for the bentonite and the bentonite-sand

Table 3. Shear Properties of the Bentonite-Sand Mixture

Bentonite	Dry Density (Mg/m ³)	Water Content (%)	Cohesion (kPa)	Angle of Friction (°)	Measuring Technique	Conditions	Ref.
Kyungju(70%)-sand (30%)	1.8	17	1100	17	triaxial	$\sigma_3=100\sim 400\text{kPa}$	3
Kyungju(50%)-sand (50%)	1.6	27	90	4	triaxial	$\sigma_3=100\sim 400\text{kPa}$	3
Kyungju(50%)-sand (50%)	1.8	17	530	6	triaxial	$\sigma_3=100\sim 400\text{kPa}$	3

Table 4. Consolidation Properties of the Compacted Bentonite and the Bentonite-Sand Mixture

Bentonite	Dry Density (Mg/m ³)	Water Content (%)	Consolidation Yield Stress (MPa)	Coefficient of Consolidation (m ² /year)	Compression Index	Ref.
Kunigel V1	1.6		1.5		0.27	25
	1.8		4.7		0.21	
Kyungju	1.8	20		0.018	0.05	3
Kunigel V1(70%) - sand(30%)	1.6		0.77		0.27	25

mixture ranges from 0.2 to 0.25 under unsaturated condition, and is 0.5 under saturated condition.

3.4. Shear Strength

The deformation of soil occurs along the surface of sliding by the shear stress of soil, and the maximum resistance to shear at the surface of sliding is a shear strength. The shear strength of soil can be expressed as a function of cohesion, internal friction angle and vertical stress.

$$S_f = ch + \sigma \tan \phi \quad (11)$$

where S_f is shear strength, ch is cohesion, ϕ is internal friction angle, and σ is vertical stress at the surface of sliding. The cohesion and the internal

friction angle for the bentonite and the bentonite-sand mixture collected from the literatures [3,11,22,23] are listed in Table 2 and Table 3. As shown in the tables, the cohesion and the internal friction angle are disposed to increase with increasing dry density of bentonite from 1.4 Mg/m³ to 1.8 Mg/m³ resulting in a increase of shear strength. The degree of increase is relatively large until the dry density of bentonite reaches 1.6 Mg/m³, and after then decreases. For the bentonite-sand mixture, the shear strength decreases slightly until the sand content reach 30 wt.%, but decreases sharply in the case of sand content of 50 wt.%. This behavior may be due to the insufficient binding force between the bentonite particles when the dry density of the mixture is low or the bentonite content is small.

3.5. Consolidation Properties

The compression of the soil volume with time due to the extrusion of pore water under load application is said to be a process of consolidation. As a clay has large void ratio and very low permeability, the settlement occurs over long period. One of the major parameters to assess the consolidation settlement is a compression index. The consolidation results plotted as void ratio versus the logarithm of effective stress show that the void ratio decreases almost linearly with increasing the logarithm of effective stress in the range of the effective stress over the pre-consolidation pressure. The slope of this type of curve is the compression index [24].

$$C_c = - \frac{\Delta e}{\Delta \log_{10} \sigma'} \quad (12)$$

where C_c is the compression index, e is the void ratio, and σ' is the effective stress. The limited data on the consolidation properties for the bentonite and the bentonite-sand mixture have been reported [3,25], and they are listed in Table 4. For the bentonite and the bentonite-sand mixture with dry density of 1.6 Mg/m³ to 1.8 Mg/m³, the compression index and the consolidation yield stress are in the range of 0.05 to 0.27, and 0.77 to 4.7, respectively. Although the collected data are limited, the compression index seems to decrease, and the consolidation yield stress seems to increase as the dry density increases. Also the consolidation yield stress of the bentonite-sand mixture is much lower than the bentonite.

4. Results of Analysis

Based on the analysis and evaluation described in the previous sections, the typical values for the

thermal and mechanical properties of the buffer material are recommended as follows:

4.1. Thermal Properties

Thermal conductivity

- bentonite

$$k = 0.0306 \omega + 0.2286 \quad (\rho_d = 1.4 \text{ Mg/m}^3)$$

$$k = 0.0345 \omega + 0.4318 \quad (\rho_d = 1.6 \text{ Mg/m}^3)$$

$$k = 0.0584 \omega + 0.4738 \quad (\rho_d = 1.8 \text{ Mg/m}^3)$$

- bentonite-sand(70:30) mixture

$$k_m = 1.5 \text{ k}$$

where k_m : thermal conductivity of the mixture (W/m °K)

k : thermal conductivity of bentonite (W/m °K)

ω : water content (%)

Specific heat

- bentonite

$$c = (32.3 + 4.18 \omega) / (100 + \omega) \quad (\rho_d = 1.8 \text{ Mg/m}^3)$$

- bentonite-sand(70:30) mixture

$$c = (34.1 + 4.18 \omega) / (100 + \omega) \quad (\rho_d = 1.6 \text{ Mg/m}^3)$$

where c : specific heat (kJ kg⁻¹, K⁻¹)

Coefficient of thermal expansion

$$\alpha = 3.1 \times 10^{-4} (1/^{\circ}\text{K}) \quad (\rho_d = 1.2 \sim 1.6 \text{ Mg/m}^3)$$

4.2. Mechanical Properties

Unconfined compression strength

- bentonite

$$\log \text{UCS} = 5.38 \times 10^{-4} \omega^2 - 0.0454 \omega + 0.3235 \quad (\rho_d = 1.4 \text{ Mg/m}^3)$$

$$\log \text{UCS} = -2.57 \times 10^{-4} \omega^2 - 0.0164 \omega + 0.3185 \quad (\rho_d = 1.6 \text{ Mg/m}^3)$$

$$\log \text{UCS} = -0.0035 \omega^2 + 0.0580 \omega + 0.5410 \quad (\rho_d = 1.8 \text{ Mg/m}^3)$$

- bentonite-sand(70:30) mixture

$$\log \text{UCS} = 0.0020 \omega^2 - 0.0930 \omega + 0.4289 \quad (\rho_d = 1.6 \text{ Mg/m}^3)$$

$$\log \text{UCS} = -0.0027 \omega^2 + 0.0107 \omega + 0.5702$$

$$(\rho_d = 1.8 \text{ Mg/m}^3)$$

where UCS : unconfined compression strength (MPa)

ω : water content (%)

Young's modulus of elasticity

- bentonite

$$\log E = 0.0038 \omega^2 - 0.1433 \omega + 2.8578$$

$$(\rho_d = 1.4 \text{ Mg/m}^3)$$

$$\log E = -3.99 \times 10^{-3} \omega^2 + 0.0593 \omega + 2.0576$$

$$(\rho_d = 1.6 \text{ Mg/m}^3)$$

$$\log E = -0.0094 \omega^2 + 0.1873 \omega + 1.6935$$

$$(\rho_d = 1.8 \text{ Mg/m}^3)$$

- bentonite-sand(70:30) mixture

$$\log E = 8.83 \times 10^{-4} \omega^2 - 0.0730 \omega + 2.3751$$

$$(\rho_d = 1.6 \text{ Mg/m}^3)$$

$$\log E = -0.0109 \omega^2 + 0.2036 \omega + 1.5275$$

$$(\rho_d = 1.8 \text{ Mg/m}^3)$$

where E : Young's modulus of elasticity
($\times 10^2$ MPa)

ω : water content (%)

Poisson ratio

: 0.05 (unsaturated condition)

$$(\rho_d = 1.4 \text{ Mg/m}^3)$$

0.22 (unsaturated condition)

$$(\rho_d = 1.6 \sim 1.8 \text{ Mg/m}^3)$$

0.5 (saturated condition)

$$(\rho_d = 1.6 \sim 1.8 \text{ Mg/m}^3)$$

Shear properties

- $\rho_d = 1.4 \text{ Mg/m}^3$
 - cohesion (kPa): 500
 - internal friction angle ($^\circ$): 27
- $\rho_d = 1.6 \text{ Mg/m}^3$
 - cohesion (kPa): 1000
 - internal friction angle ($^\circ$): 37
- $\rho_d = 1.8 \text{ Mg/m}^3$
 - cohesion (kPa): 1100
 - internal friction angle ($^\circ$): 50

The recommended values for the thermal and mechanical properties of the buffer material can be useful for the preliminary assessment of the alternatives for the design concept of a high-level waste repository in Korea. However in future, when the repository design concept would be fixed and the detailed performance assessment is required, the extensive direct measurements of the thermal and mechanical properties of the domestic bentonite should be performed.

5. Conclusions

The thermal and mechanical property of the compacted bentonite and the mixture of bentonite and sand collected from the literatures show a similar trend although spread in the data due to the difference between the type of bentonite and the measuring techniques exists. The thermal conductivity of bentonite is found to increase almost linearly with increasing dry density of the bentonite. In the case of constant dry density, the thermal conductivity is proportional linearly to the water content. The specific heat can also be expressed as a function of water content, and the coefficient of thermal expansion is almost constant. The logarithm of unconfined compressive strength and Young's modulus of elasticity increases linearly with increasing dry density, and in the case of constant dry density, it can be fitted to a second order polynomial of water content. Also the unconfined compressive strength and Young's modulus of elasticity of the bentonite-sand mixture decrease with increasing sand content. The Poisson's ratio remains constant at the dry density higher than 1.6 Mg/m^3 , and the shear strength increases with increasing dry density. Using these results, the typical values of thermal and mechanical properties of the bentonite and the bentonite-sand mixture are suggested. These results could be useful for the

preliminary assessment of the performance of the engineered barriers in a high-level waste repository.

References

1. G.R. Simmons and P. Baumgartner, "The disposal of Canada's nuclear fuel waste: engineering for a disposal facility," Atomic Energy of Canada Limited Report, AECL-10715, COG-93-5 (1994).
2. SKBF/KBS, "Final storage of spent fuel - KBS-3" (1983).
3. W.J. Cho, J.O. Lee, C.H. Kang, and K.S. Chun, "Physicochemical, mineralogical and mechanical properties of domestic bentonite and bentonite-sand mixture as a buffer material in the high-level waste repository," KAERI/TR-1388/99. Korea Atomic Energy Research Institute (in Korean) (1999).
4. L. Börjesson, A. Fredrikson, and L.-E. Johannesson, "Heat conductivity of buffer materials," SKB Technical Report 94-29 (1994).
5. H. S. Radhakrishna, "Thermal properties of clay-based buffer materials for a nuclear fuel waste disposal vault," AECL-7805 (1984).
6. J. G. Hartley and W. J. Black, "Transient simultaneous heat and mass transfer in moist, unsaturated soils," J. of Heat Transfer, Transaction of the ASME, 103, 376 (1981).
7. JNC, "H12 Project to establish technical basis for HLW disposal in Japan," Supporting Report 2, Japan Nuclear Cycle Development Institute, Japan (1999).
8. M. Kumata, S. Muraoka, K. Shimooka, M. Okamoto, and K. Araki, "In situ buffer material test (I)- Compacted bentonite," JAERI-M 87-164, Japan Atomic Energy Research Institute (in Japanese) (1987).
9. M. Kumata, A. Nakagoshi, K. Shimooka, S. Muraoka, and H. Nakamura, "In situ buffer material test (II)- A preliminary test on a bentonite/sand mixture," JAERI-M 87-171, Japan Atomic Energy Research Institute (in Japanese) (1987).
10. S. Knutsson, "On the thermal conductivity and thermal diffusivity of highly compacted bentonite," SKB Technical Report 83-72 (1983).
11. L. Börjesson, H. Hokmark, and O. Karnland, "Rheological properties of sodium smectite clay," SKB Technical Report 88-30 (1988).
12. A. Beziat, M. Dardaine, and V. Gabis, "Effect of compaction pressure and water content on the thermal conductivity of some natural clays," Clays and Clay Minerals, 36, 462-466 (1988).
13. H. Suzuki, M. Shibata, J. Yamagata, I. Hirose, and K. Terakado, "Physical and mechanical properties of bentonite (I), PNC TN8410 92-057 (in Japanese) (1992).
14. K.S. Chun, W.J. Cho, J.O. Lee, S.S. Kim, and M.J. Kang, "High-level waste disposal technology development- Development of engineered barrier," KAERI/RR-1897/98. Final Report, MOST (in Korean) (1998).
15. E. Mingaro et al., "Characterization of clay(bentonite)/crushed granite mixtures to build barrier against the migration of radionuclides: diffusion studies and physical properties," EUR 13666 EN, Commission of the European Communities (1990).
16. H. Suzuki, M. Shibata, J. Yamagata, I. Hirose and K. Terakado, "Physical and mechanical properties of bentonite (II), PNC TN8410 92-057, Power Reactor and Nuclear Fuel Development Corporation (in Japanese). (1992).
17. K. Takaji and H. Suzuki, "Static mechanical properties of buffer material," Japan Nuclear Cycle Development Institute, JNC-TN8400 99-

- 041, Japan Nuclear Fuel Cycle Development Institute (in Japanese) (1999) .
18. T. Fujita, A. Saotome, K. Hara, "Mechanical properties of buffer material," PNC TN8410 92-170, Power Reactor and Nuclear Fuel Development Corporation (in Japanese) (1992) .
19. M. Maeda, K. Tanai, M. Ito, M. Mihara, and M. Tanaka, "Mechanical properties of the Ca-exchanged and Ca bentonite", PNC TN8410 98-021, Power Reactor and Nuclear Fuel Development Corporation (in Japanese) (1998).
20. K. Takaji and W. Taniguchi, "Dynamic mechanical properties of buffer material," Japan Nuclear Cycle Development Institute, JNC Technical Report, JNC-TN8400 99-042 (in Japanese) (1999).
21. M. Maeda, M. Ito, M. Mihara, and M. Tanaka, "Consolidated undrained triaxial test of the Ca-exchanged bentonite," PNC TN8410 97-314, Power Reactor and Nuclear Fuel Development Corporation (in Japanese) (1997).
22. E. Mingaro et al., "Characterization of clay(bentonite)/crushed granite mixtures to build barrier against the migration of radionuclides: diffusion studies and physical properties," EUR 13666 EN, Commission of the European Communities (1990).
23. L. Börgesson and R. Pusch, "Rheological properties of calcium smectite," SKB Technical Report 87-31 (1987).
24. T. W. Lambe, R. V. Whitman, Soil Mechanics, John Wiley and Sons, New York, (1969).
25. T. Namikawa and T. Kanno, "Consolidation properties of buffer materials," Power Reactor and Nuclear Fuel Development Corporation, PNC TN8410, 97-051 (in Japanese) (1997).
26. W. J. Cho, J. O. Lee and C. H. Kang, "A compilation and evaluation of thermal and mechanical properties of compacted bentonite for the performance assessment of engineered barriers in the high-level waste repository," Korea Atomic Energy Research Institute, KAERI/TR-1826/2001 (in Korean) (2001).